Taylor & Francis
Taylor & Francis Group

Journal of Energetic Materials

ISSN: 0737-0652 (Print) 1545-8822 (Online) Journal homepage: http://www.tandfonline.com/loi/uegm20

A Study of the Detonation Behavior of an Annular Booster Pellet

Zhong-Qing Xue, Shuang-Qi Hu, Xiong Cao & Jun Zhang

To cite this article: Zhong-Qing Xue, Shuang-Qi Hu, Xiong Cao & Jun Zhang (2016): A Study of the Detonation Behavior of an Annular Booster Pellet, Journal of Energetic Materials, DOI: 10.1080/07370652.2016.1139640

To link to this article: http://dx.doi.org/10.1080/07370652.2016.1139640

Published online: 05 Apr 2016.

JOURNAL OF ENERGETIC MATERIALS
http://dx.doi.org/10.1080/07370652.2016.1139640

A Study of the Detonation Behavior of an Annular Booster Pellet

Zhong-Qing Xue[a], Shuang-Qi Hu[a], Xiong Cao[a], and Jun Zhang[b,c]

[a]Chemical Industry and Ecology College, North University of China, Taiyuan, P.R. China; [b]Chemical Industry and Ecology College, North University of China, Taiyuan, P.R. China; [c]Hubei Space Sanjiang Honglin Detection and Control Co., Ltd. Hubei, P.R. China

ABSTRACT
An annular-shaped booster pellet has been developed in order to study the capability of such a design to initiate the detonation of insensitive high explosives (IHE). The detonation characteristics of an annular booster design were studied theoretically by numerical simulation and experimentally. Results showed that if the annular booster pellet were detonated simultaneously at four symmetrical points, the detonation wave collision could be achieved within the pellet. The pairs of impacts of the four detonation wavefronts generated enhanced shock pressures in four radially symmetric directions. The tangential energy flow from the collision of detonation plays a major part in improving the initiation capability of an annular booster pellet. The numerical simulation is qualitatively consistent with the experimental results.

KEYWORDS
Annular booster pellet; detonation wave collision; tangential energy flow; initiation capability; overdriven detonation

Introduction

The initiating capability of boosters needs to be increased due to their wide chemical reaction zone, long reaction time, and high critical initiating pressure of insensitive high explosives (IHE). Traditional cylindrical booster pellets have had to be modified to ensure the reliable initiation of IHE. There has been a gradual emergence of specially shaped structures, initiation mode diversification, and converging output energy (Chou, Roslund, and Liang 1993; Ferm and Hull 1993; Grattan et al. 2006; Mader 2007; Hu et al. 2014a, 2014b; Kozlov, Ol'khov, and Shuvalova 2015) in booster design. In 1978, a system was described that required three detonation trains to be freed simultaneously to detonate a PBX 9407 acceptor charge (Goforth 1978). In 1980, the flow resulting from the interaction of three spherically diverging detonation waves was examined by using the three-dimensional Eulerian hydrodynamic computer code (Mader and Kershner 1980). In 1981, the heterogeneous explosive shock initiation processes by single-wave (Bowman and Mader 1981) and triple-wave interaction from three initiators (Mader and Kershner 1981a) were described by using the two-dimensional Lagrangian code or three-dimensional Eulerian hydrodynamic code with the Forest Fire rate. The effect of multipoint initiation of an explosive on the motion of a thin metal plate was investigated in two-dimensional geometry. Four spherically diverging detonation waves were modeled by using the three-dimensional reactive hydrodynamic code consisting of four detonators (Mader and Kershner 1981b).

Recently, our group has designed annular booster pellets based on the analysis of shock initiation theory of explosives, and the initiation processes were simulated using ANSYS/LS-DYNA software (Livermore Software Technology Corporation [LSTC]). Experimental measurements were performed

CONTACT Zhong-Qing Xue xzq2701@163.com Chemical Industry and Ecology College, North University of China, Taiyuan, P.R. China 030051.

Color versions of one or more of the figures in this article can be found online at www.tandfonline/uegm.

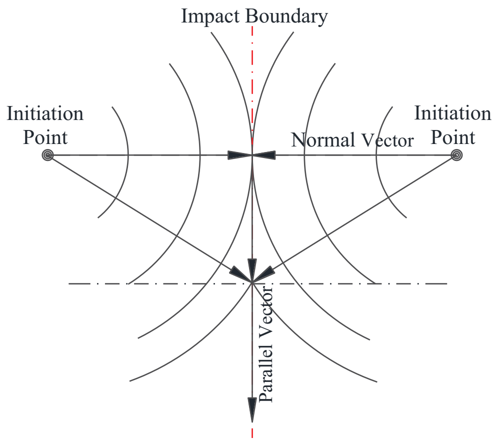

Figure 1. Oblique collision of two identical detonation waves.

to test the initiation capacities. The results showed that the annular structures can increase the initiation capability of boosters (Hu, Hu, and Cao 2012, 2013).

Head-on collision and oblique collision will occur when two detonation waves collide with each other. The oblique collision is formed when an incidence angle is not equal to zero. In this case, the pressure at the collision point would increase sharply (Dunne 1964; Pratt, Humphrey, and Glenn 1991). When the oblique collision occurs, a beam of waves that pass through the initiation point and collision point can be divided into two orthogonal vectors: normal and parallel (see Fig. 1). The former means that the vector is perpendicular to the impact boundary and the latter that it is parallel to it. Because the parallel vector is parallel to the tangent at the head-on collision point, the energy transmitted by the detonation products along this tangential direction was defined as the tangential energy flow in this work.

There have been many earlier studies on the initiation capability of annular booster pellets. However, to our knowledge, no theoretical or experimental investigations into the effect of tangential energy flow on the initiation capability of annular booster pellets were performed.

In this work, the annular booster pellet was chosen as a research subject in order to evaluate the effect of tangential energy flow on the initiation capability. Different sections of the detonation waveform and its associated pressure changes in the whole shock-to-detonation transition were simulated using ANSYS/LS-DYNA software. The mechanical behavior of the tangential energy flow was studied using a steel witness plate.

Numerical simulation

Detonation wave collision 2D model

Throughout the whole shock-to-detonation transition, it is assumed that the detonation waveform in the booster is similar to that in the main charge and that the wave is spherical. The radial 2D section is shown in Fig. 2. In Fig. 2, the hatched area means the booster, the shaded area means the main charge, and the arrow means tangential direction at the head-on collision point.

Building of solid model

Three-dimensional, co-node, and quarter-symmetry models were developed with meshing techniques using a finite element preprocessor module of ANSYS14.5. To reduce the effects of grid precision on the accuracy of simulation results (Short and Quirk 1997), the grid size was chosen

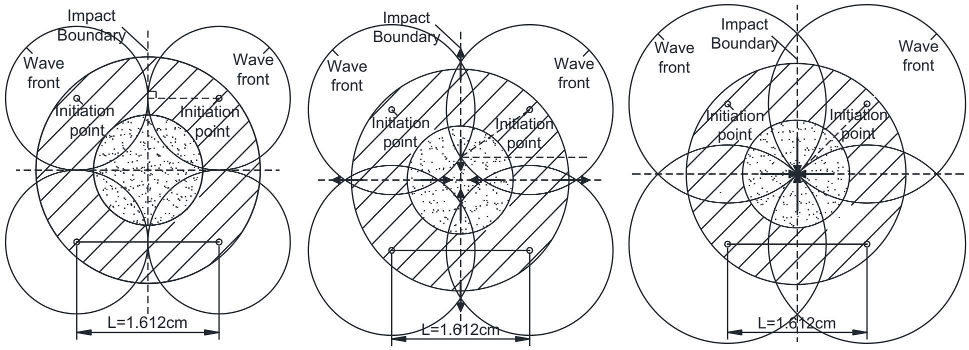

Figure 2. Radial 2D model of an annular booster pellet shock initiation process.

to be 1.25×10^{-4} m. The dimension was kilogram, meter, and second. The grid and geometric models are shown in Figs. 3 and 4:

In Fig. 4, Part 1 is the primary explosive pellet. Part 2 is the annular booster pellet, and the material is LX-10. Part 3 is the main charge, and the material is TNT. The inner diameter, outer diameter, and height of the annular booster pellet are 1.90, 2.90, and 2.00 cm, respectively. The diameter and height of the main charge pellet are 1.90 and 2.00 cm, respectively. The element from point O to point O′ is represented by O → O′. Points E and E′ are the midpoints of the arcs AC and A′C′, respectively. Points F and F′ are the midpoints of the arcs BD and B′D′, respectively.

Material models

The primary explosive was characterized by the model of the detonation of a generalized high explosive and the Jones-Wilkins-Lee equation. The booster detonation was modeled using a trinomial approximation to the initiation growth model widely used in fluid dynamics calculations (Lee and Tarver 1980). The properties of LX-10 (Tarver et al. 1993; Vandersall et al. 2007) were used for

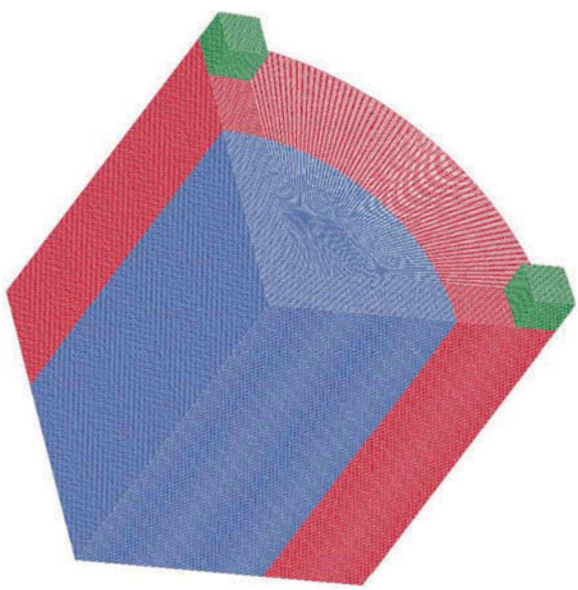

Figure 3. Entities grid model.

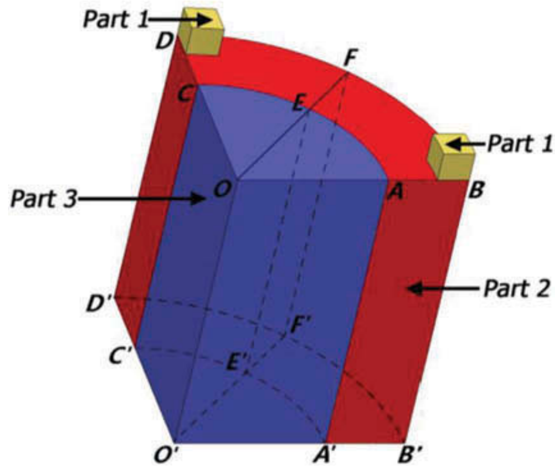

Figure 4. Geometric model.

simulation of the booster. In order to obtain a better waveform in the whole detonation wave propagation, TNT was used for the Part 3 material. The trinomial approximation to the ignition growth model was also used for TNT and its parameters are available in the literature (Lee and Tarver 1980).

Simulation results and discussion

LS-DYNA/v971.exe solvers (LSTC) were used for the solution, LS-PrePost-4.0 postprocessing software (LSTC) was used for data acquisition, and Origin 9.0 Data analysis software (OriginLab Corporation) was used to organize the data. The results of the numerical simulation are shown in Figs. 5–9.

In Fig. 8, curve (1) means the maximal pressures of all elements of the booster, and the pressures in the detonation state in the Chapman-Jouguet plane were determined using curve (2). In the annular booster pellet, curve (1) shows a gradual rise in pressure from 1.0 to 1.6 μs. This trend is obvious because when the detonation wave propagated toward the center, the unreacted explosive was compressed gradually in front of the wavefront. In the state after the wave was strengthened, the wave velocity accelerated and gradually transformed to a wave of

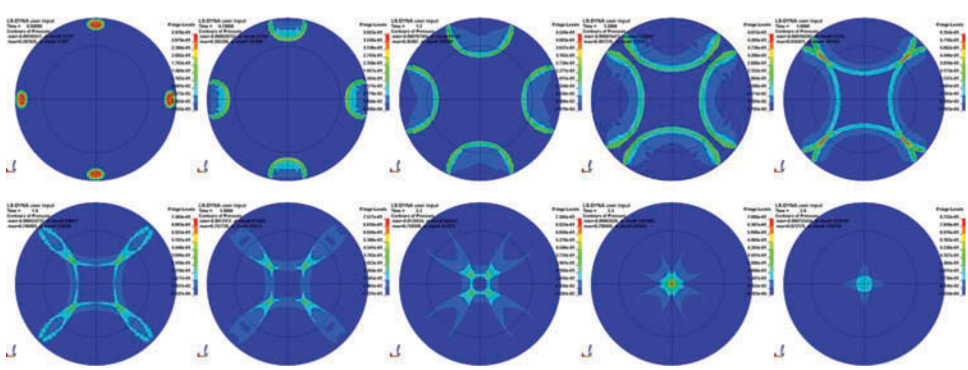

Figure 5. Pressure change in a radial section.

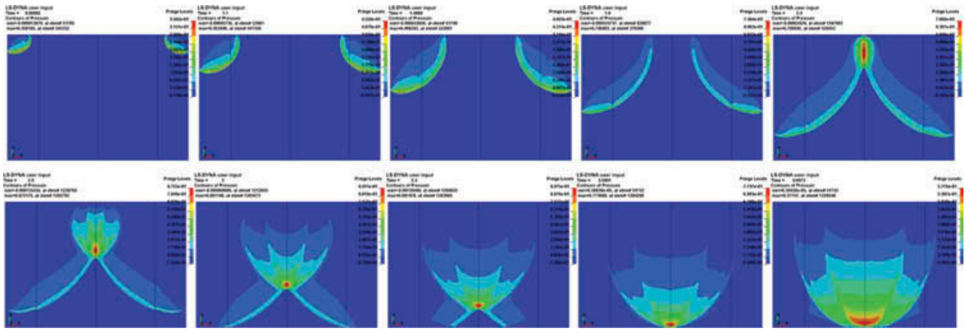

Figure 6. Pressure change in the section through the initiation point and the central axis.

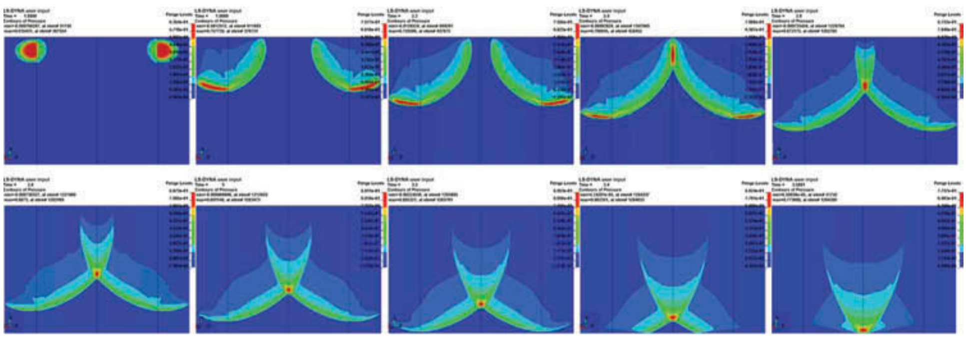

Figure 7. Pressure change in the section through the collision point and the central axis.

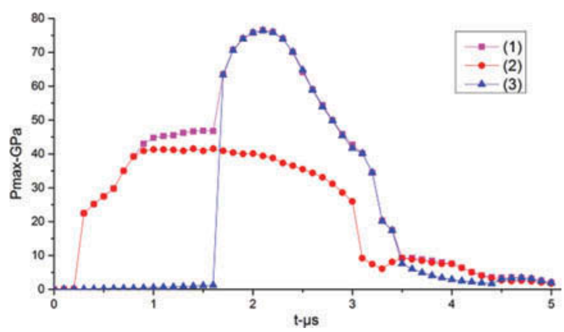

Figure 8. $P_{max} - t$ plot for the annular booster pellet: (1) all elements of the booster, (2) element AA′B′B of the booster, (3) element EE′F′F of the booster, (4) all elements of the charge, (5) element OO′A′A of the charge, (6) element OO′E′E of the charge, and (7) axis OO′ of the charge element.

detonation state above the Chapman-Jouguet detonation point (overdriven detonation; Kineke and West 1970; Fritz et al. 1996; Tang 1998). Indeed, from 0.9 μs, curve (1) is obviously above curve (2). At about 1.7 μs, curve (3), which denotes the pressure of the collision surface EE′F′F, increased rapidly and overlapped with curve (1), indicating that collision occurred between two detonation waves. The maximal pressure at the head-on collision point reached about 60 GPa at about 1.7 μs. Then and oblique collision occurred. The pressure in the oblique collision was higher than that at the head-on collision point, consistent with previous investigations (Mader and Venable 1979; Mader 2007). From Fig. 8, curve (3) is continuously increasing after 1.7 μs.

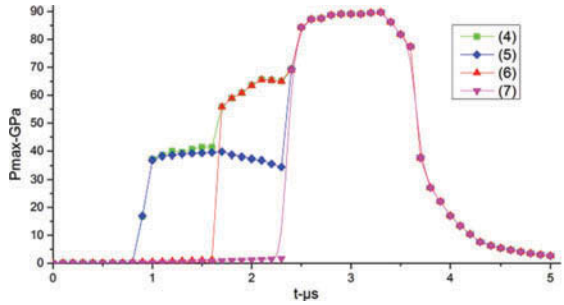

Figure 9. $P_{max} - t$ plot for the main charge: (1) all elements of the booster, (2) element AA′B′B of the booster, (3) element EE′F′F of the booster, (4) all elements of the charge, (5) element OO′A′A of the charge, (6) element OO′E′E of the charge, and (7) axis OO′ of the charge element.

From 1.7 to 3.0 μs, the average pressure on the collision surface EE′F′F is about 65 GPa, which is nearly 25 GPa more than that on surface AA′B′B.

As can be seen from Fig. 9, in the main charge, at 1.7 μs the pressure on collision surface OO′E′E is about 50 GPa, which is about two times of that on surface OO′A′A. From 1.7 to 2.4 μs, the average pressure on collision surface OO′E′E is about 55 GPa, which is nearly 29 GPa more than that on surface OO′A′A. At 2.4 μs the waves arrive at the axis. It is evident from Fig. 5 that the velocity of tangential energy flow is higher than that of the detonation wavefront and thus the energies taken by the collision surfaces and detonation wavefronts are translated into the axis at the same time and the pressures are greatly enhanced at the axis.

In summary, in the annular booster pellet, the pressures on the collision surface are greater than that on the initiation surface after 1.7 μs, as is also found in the main charge. Therefore, the tangential energy flow from the collision of the detonation waves played a notable part in improving the initiating capability of the annular booster pellet. In other words, the presence of the overdriven detonation state is vital in explaining agreement between theoretical and experimental results.

Experimental

Experimental conditions

1. Preparation of the booster pellets: Plastic-bonded explosive LX-10 was used as the booster. The annular booster pellets were pressed by external positioning of the mold, and the density was 1.658 g/cm^3. The inner diameter, outer diameter, and height of the annular booster pellet were 1.90, 2.90, and 2.00 cm, respectively. The annular booster pellet is shown in Fig. 10.

2. Preparation of the four-point synchronous explosive circuits: Ultrafine cyclotetramethylenetetranitramine (HMX) was adopted for the circuit charge. The charge densities were in the range of 0.95–1.10 g/cm^3. The height was 0.3 cm. The other dimensions are shown in Fig. 11a. Its upper end

Figure 10. Annular booster pellets.

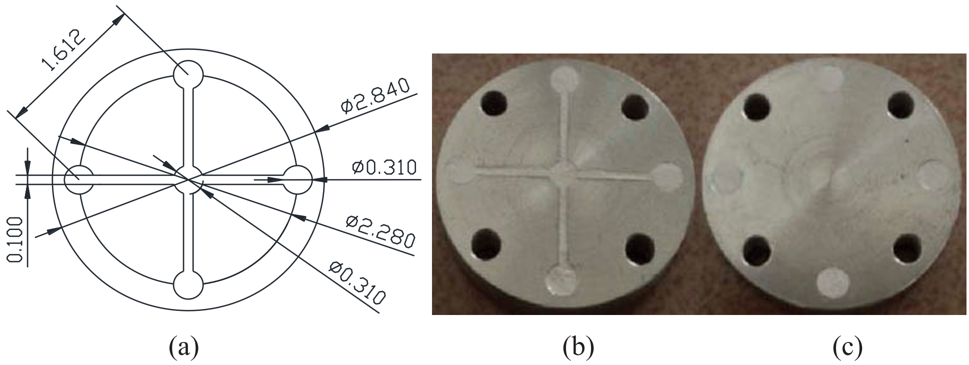

Figure 11. Four-point synchronous explosive circuit (unit: centimeters).

surface (see Fig. 11b) was in contact with the detonator. Its lower end surface (see Fig. 11c) was in contact with the annular booster pellet.

3. Selection of steel witness plate: Three structures of steel witness plates were selected. They were made from general carbon steel (1045). The inner diameter, outer diameter, and height of the lateral steel witness plate were 2.90, 10.00, and 2.00 cm, respectively. The lateral steel witness plate is shown in Fig. 12. The diameter and height of the central steel witness plate were 1.90 and 1.35 cm, respectively. The central steel witness plate is shown in Fig. 13. The diameter and height of the axis steel witness plate were 10.00 and 5.00 cm, respectively.

Experimental device

An experimental device was used to measure the initiation capability of the annular booster pellet. The details of this device are shown in Figs. 14 and 15.

Experimental results and discussion

The tangential energy flow from the annular booster pellet was studied by means of a lateral steel witness plate, and the initiation point outside the lateral steel witness plate was labeled. The lateral steel witness plate was cut into four parts by the shock impact of the detonation wave (see Fig. 16a), and obvious cutting grooves were found inside of the plate (see Fig. 16b). The incisions were located in between every two initiation points, and the angles between every two neighboring incisions were about 90° (see Fig. 16a). This is perhaps because the temperatures and pressures from tangential

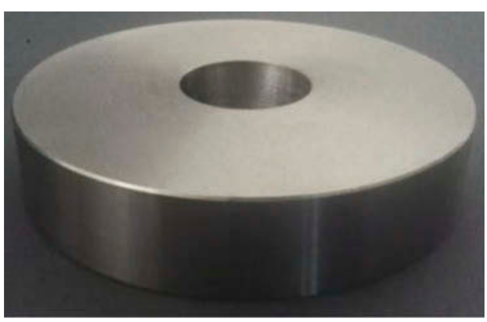

Figure 12. Lateral steel witness plate.

Figure 13. Central steel witness plate.

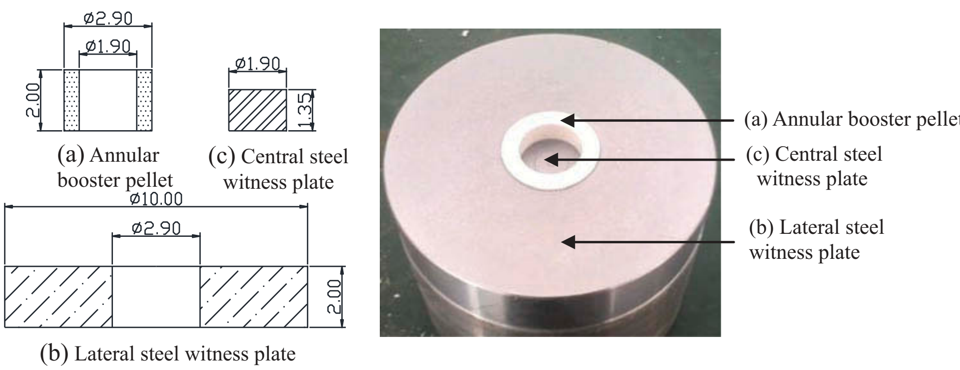

Figure 14. Relative locations of the annular booster pellet, the central steel witness plate, and the lateral steel winess plate (cm).

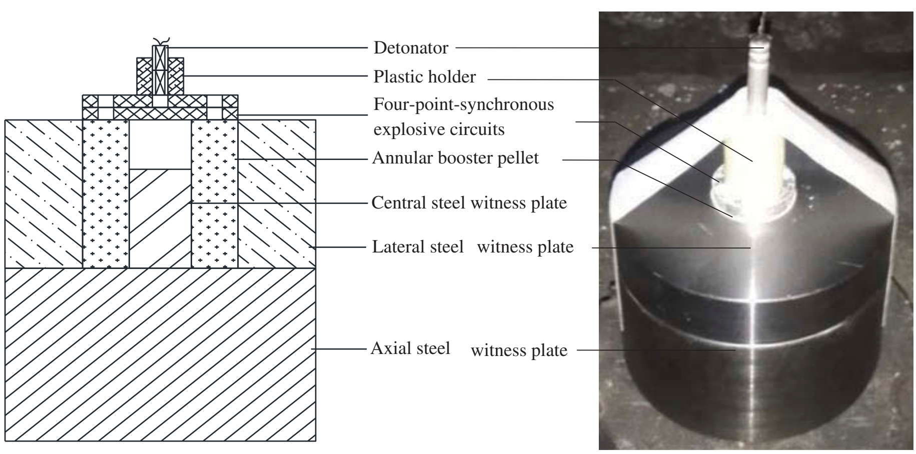

Figure 15. Experimental device (annular booster pellet under four-point synchronous explosive circuit).

Figure 16. Experimental result for the lateral steel witness plate.

energy flow in the overdriven detonation state are higher than those in the detonation wavefront, leading to the formation of the cutting grooves. Then the explosion products expanded outwards and the high-strain-rate tensile strength was exceeded in the cutting groove, leading to the formation of four parts. This not only confirmed the simulation results but showed that the effect of the tangential energy flow cannot be neglected in the structural design of booster pellets of this type.

The measurements of the central witness plate were as follows: the axis height was 1.13 cm, the margin height was 1.66 cm, and the average diameter was 1.78 cm (see Fig. 17). When these measurements were compared to those of the central witness plate before the experiment, it was found that the axial height was reduced by 0.22 cm, the margin height was increased by 0.31 cm, and diameter was reduced by 0.12 cm. The central steel witness plate was still cylindrical in shape but had four grooves on its outside. This is perhaps due to the higher temperatures and pressures in the tangential energy flow than those in the other directions, in agreement with the simulation results.

Figure 17. Experimental result for the central steel witness plate.

Conclusions

In this work, the effect of tangential energy flow on the initiation capability of the annular booster pellets was investigated using arbitrary Lagrange-Euler simulation and mechanical behavior of the tangential energy flow in the steel witness plate. The results showed that after four-point detonation of the annular booster pellet, collision of the detonation waves occurred inside the pellet and generated tangential energy flow in the tangential direction at the head-on collision point. The tangential energy flow from the collision of detonation waves played a notable part in improving the initiating capability of the annular booster pellet. The effect of the tangential energy flow cannot be neglected in the structural design of booster pellets. The description of qualitative features by the numerical simulation is consistent with the experimental results.

References

Bowman, A. L. and C. L. Mader. 1981. Numerical modeling of insensitive high-explosives initiation. Report No. LA-8437. Los Alamos, NM: Los Alamos National Laboratory.

Chou, P. C., L. Roslund, and D. Liang. 1993. Impact initiated annular retonation wave in explosive. *Propellants, Explosives, Pyrotechnics* 18 (5):264–269. doi:10.1002/(ISSN)1521-4087.

Dunne, B. 1964. Mach reflection of detonation waves in condensed high explosives. II. *Physics of Fluids (1958–1988)* 7 (10):1707–1712. doi:10.1063/1.1711077.

Ferm, E. N., and L. M. Hull. 1993. *Reflected-Shock Initiation of Explosives*. Los Alamos, NM: Los Alamos National Laboratory.

Fritz, J. N., R. S. Hixson, M. S. Shaw, C. E. Morris, and R. G. McQueen. 1996. Overdriven-detonation and sound-speed measurements in PBX-9501 and the “thermodynamic” Chapman–Jouguet pressure. *Journal of Applied Physics* 80 (11):6129–6141. doi:10.1063/1.363681.

Goforth, J. H. 1978. Safe-stationary detonation train for Army ordnance. Report No. LA-7123. Los Alamos, NM: Los Alamos National Laboratory.

Grattan, A. F., M. L. Patterson, J. M. Barker, and T. J. Wuensche. 2006. *Apparatus and Method for Severing Pipe Utilizing a Multi-point Initiation Explosive Device*. U.S. Patent 7,104,326.

Hu, L. S., S. Q. Hu, and X. Cao. 2012. Study on the initiation capacities of two booster pellets. *Central European Journal of Energetic Materials* 9 (3):261–272.

Hu, L. S., S. Q. Hu, and X. Cao. 2013. Application of the multipoint synchronous circuit of the annular booster pellet. *International Journal of Energetic Materials and Chemical Propulsion* 12 (6):475–485. doi:10.1615/IntJEnergeticMaterialsChemProp.v12.i6.

Hu, L. S., S. Q. Hu., X. Cao, and J. R. Zhang. 2014a. Initiation capacity of a specially shaped booster pellet and numerical simulation of its initiation process. *Journal of Energetic Materials* 32 (1):27–36. doi:10.1080/07370652.2012.731134.

Hu, S. Q., H. R. Liu, L. S. Hu, X. Cao, X. C. Mi, and H. X. Zhao. 2014b. Study on the structures of two booster pellets having high initiation capacity. *Journal of Energetic Materials* 32 (Suppl. 1):S3–S12. doi:10.1080/07370652.2013.812161.

Kineke, J. H., and C. E. West. 1970. Shocked states of four overdriven explosives. Proceedings of the 5th International Symposium on Detonation, August 18–21, Pasadena, CA, USA.

Kozlov, E. A., O. V. Ol’khov, and E. V. Shuvalova. 2015. Numerical 3D-modeling of spall and shear fractures in shells of austenitic 12Kh18N10T steel and 30KhGSA steel under their spherical and quasi-spherical explosive loading. *International Journal of Modeling, Simulation, and Scientific Computing* 6 (1):1550011. doi:10.1142/S1793962315500117.

Lee, E. L., and C. M. Tarver. 1980. Phenomenological model of shock initiation in heterogeneous explosives. *Physics of Fluids (1958–1988)* 23 (12):2362–2372. doi:10.1063/1.862940.

Mader, C. L. 2007. *Numerical Modeling of Explosives and Propellants*. CRC Press.

Mader, C. L. and J. D. Kershner. 1980. Three-dimensional Eulerian calculations of triple-initiated PBX 9404. Report No. LA-8206. Los Alamos, NM: Los Alamos National Laboratory.

Mader, C. L. and J. D. Kershner. 1981a. Three-dimensional modeling of triple-wave initiation of insensitive explosives. Report No. LA-8655. Los Alamos, NM: Los Alamos National Laboratory.

Mader, C. L. and J. D. Kershner. 1981b. Two- and three-dimensional detonation wave interactions with a copper plate. Report No. LA-8989. Los Alamos, NM: Los Alamos National Laboratory.

Mader, C. L. and D. Venable. 1979. Mach stems formed by colliding cylindrical detonation waves. Report No. LA-7869. Los Alamos, NM: Los Alamos National Laboratory.

Pratt, D. T., J. W. Humphrey, and D. E. Glenn. 1991. Morphology of standing oblique detonation waves. *Journal of Propulsion and Power* 7 (5):837–845. doi:10.2514/3.23399.

Short, M. and J. J. Quirk. 1997. On the nonlinear stability and detonability limit of a detonation wave for a model three-step chain-branching reaction. *Journal of Fluid Mechanics* 339:89–119. doi:10.1017/S002211209700503X.

Tang, P. K. 1998. *A Study of the Overdriven Behaviors of PBX 9501 and PBX 9502*. Los Alamos, NM: Los Alamos National Laboratory.

Tarver, C. M., P. A. Urtiew, S. K. Chidester, and L. G. Green. 1993. Shock compression and initiation of LX-10. *Propellants, Explosives, Pyrotechnics* 18 (3):117–127. doi:10.1002/(ISSN)1521-4087.

Vandersall, K. S., C. M. Tarver, F. Garcia, P. A. Urtiew, and S. K. Chidester. 2007. Shock initiation experiments on the HMX based explosive LX-10 with associated ignition and growth modeling. Proceedings of the 14th American Physical Society Topical Conference on Shock Compression of Condensed Matter, June 24–29, Waikoloa, HI.